SBF
SOCIEDADE BRASILEIRA DE FÍSICA

GENERAL AND APPLIED PHYSICS

Check for updates

A Paper-Based Colorimetric Sensor for Highly Sensitive and Selective Detection of Multi-metal Ions in Water

Anoop Singh[1] · Prerna Mahajan[1] · Asha Sharma[1] · Aamir Ahmed[1] · Sonali Verma[1] · Bhavya Padha[1] · Sandeep Arya[1]

Abstract

In this article, we present a $NaYF_4$:Eu^{3+}-based ultrasensitive colorimetric detection technique and demonstrate its successful implementation for the detection of four metal ions in water. The developed colorimetric sensors demonstrated exceptional stability in 100% aqueous solution and showed distinct absorption spectrum signals and significant color differences for Cu^{+2}, Mn^{+2}, Co^{+2}, and Mo^{+4}. Additionally, an attempt is made to detect heavy metal ions from mixtures of two or three metals. In that scenario, we also noticed distinct colors for distinct combinations. A simple test strip was developed for visual monitoring of four metal ions with a detection limit approximated by the naked eye. This suggested that colorimetric approach enables fast, sensitive, and portable detection of various metal ions, indicating a significant potential for on-site rapid water quality analysis.

Keywords Sensor · Nanostructure · Water · Optical properties · Absorption

1 Introduction

In the twenty-first century, the safety and maintenance of the quality of drinking water are a great challenge. Water is important for all living beings on earth, and its quality has decreased significantly due to chemical pollutants. Due to increased industrial and agricultural expansion in recent years, large amounts of hazardous and carcinogenic heavy metal ions have been discharged into the environment [1–3]. Mining and sewage discharge have also led to an increase in the concentration of heavy metal ions in water [4–6]. The heavy metals have high atomic weight and density. These are non-biodegradable, possess high solubility in water, and get easily absorbed into the living organisms. Heavy metals are considered the major chemical pollutants and have existed since centuries. Cross-contamination of heavy metals, which involves the presence of numerous or even distinct species of harmful heavy metal ions, is also becoming more prevalent in hydrological environments [7], posing a major hazard to ecological systems and organisms [8]. The heavy metals include arsenic (As), lead (Pb), mercury (Hg), nickel (Ni), zinc (Zn), cadmium (Cd), cerium (Ce), chromium (Cr),

manganese (Mn), molybdenum (Mo), copper (Cu), iron (Fe), etc. [9, 10]. Some of the heavy metal ions like chromium (III) and iron are required by the living organisms in traces, but an increased intake leads to serious consequences. Heavy metals when accumulated in the human body can cause cancer and damage the liver, kidney, lungs, reproductive system, DNA, etc. [11, 12]. Long exposure to heavy metal ions has also resulted in diseases like minimata and Parkinson's disease [11]. As a result, precise identification and quantification of heavy metal ions, as well as their speciation, are critical. However, the complicated hydrological environment makes it extremely difficult to detect and analyze groundwater contamination effectively [13]. The high solubility of these metals in water also adds to the problem. Existing analysis techniques, like atomic absorption, emission, and mass spectroscopy, are dependent on costly and time-consuming field sampling and laboratory testing procedures [14], which place stringent requirements on the storage and transportation of delicate water samples. Additionally, the majority of detection techniques are capable of measuring only the overall concentration of metal ions, whereas speciation analysis involves extensive pretreatments such as oxidation, reduction, or the inclusion of additives [15]. These techniques are also time-consuming, costly, and require expertise. The development of a unique detection method capable of rapid, simple, and portable on-site recognition of numerous metal ions and polyvalent metal speciation

✉ Sandeep Arya
snp09arya@gmail.com

1 Department of Physics, University of Jammu, Jammu, Jammu and Kashmir 1800006, India

analysis is critical. Colorimetric approaches have emerged as a viable alternative to spectroscopy-based methods due to their ease of use, low cost, and rapid response time [16]. Colorimetric detection of metal ions can be detected directly with the naked eye or monitored using a portable UV–vis spectrophotometer, eliminating the need for time-consuming instrumental analysis [17]. The colorimetric probe of tiny molecules, in particular, sparked increased interest since it contains several recognition sites and is capable of concurrently recognizing different metal ions.

Herein, we provide an ultrasensitive colorimetric detection approach based on $NaYF_4:Eu^{3+}$ and illustrate its successful application to the detection of four metal ions, i.e., Cu^{+2}, Mn^{+2}, Co^{+2}, and Mo^{+4} in water. Additionally, heavy metal ions are also detected in combination of two or three metals. A simple test strip with a detection limit approximated by the naked eye was created for visual monitoring of four metal ions. This study demonstrated a rapid and ultrasensitive detection of a variety of metal ions, implying a substantial potential for on-site speedy water quality examination.

2 Material and Methods

2.1 Synthesis of NaYF₄:Eu Nanoparticles

For the synthesis of $NaYF_4:Eu$ nanoparticles, yttrium oxide (Y_2O_3), europium oxide (Eu_2O_3), sodium fluoride (NaF), and hydrochloric acid (HCl) were used as precursor materials. 1.45 g Y_2O_3 in 32 ml HCl and 0.56 g Eu_2O_3 in 8 ml HCl were dissolved under constant stirring and heating in two separate beakers. Afterwards, mixing of both the solutions was done followed by the addition of 40 ml EDTA. Ammonia solution was added dropwise for maintaining pH 2. This solution was poured into 120 ml NaF solution and left undisturbed for 1 h. Centrifugation was performed to collect the nanoparticles, which were then washed several times with deionized water and ethanol and dried in an oven at 95 °C.

3 Results and Discussion

3.1 Structural Characterization

Synthesized $NaYF_4:Eu$ nanoparticles exhibited the XRD pattern as displayed in Fig. 1a. The peaks of $NaYF_4:Eu$ have been observed at 2θ angles of 29.22°, 31.74°, 45.5°, 46.61°, 52.84°, 53.71°, 54.35°, 55.04°, and 58.01° corresponding to (110), (101), (201), (210), (002), (300), (211), (102), and (301) planes. Due to the sharpness of the XRD peaks, the produced nanoparticles were determined to be

highly crystalline [18, 19]. According to the JCPDS File No. 28–1192, the relative intensity and position of all diffraction peaks could be easily correlated to the pure hexagonal NaYF4 [20]. The result indicates that the sol–gel approach is suitable for the preparation of doped $NaYF_4$ nanoparticles with a pure hexagonal phase. The crystallite size is calculated using Debye–Scherrer equation as shown in Eq. (1).

$$D = 0.9\lambda/\beta cos\theta \tag{1}$$

where D, λ, β, and 2θ represent the average crystallite size, X-ray wavelength, full width half maxima, and diffraction angle, respectively [21]. As computed from the aforementioned equation, the average crystallite size of the prepared $NaYF_4:Eu$ nanoparticles is roughly 60 nm.

3.2 Morphological Characterization

FESEM image of $NaYF_4:Eu$ nanoparticles is shown in Fig. 1b. The image clearly shows that the prepared nanoparticles have a spherical shape and a uniform size. The acquired results are consistent with the average particle size determined by XRD analysis. The results demonstrate that $NaYF_4:Eu$ nanoparticles are formed successfully.

3.3 Elemental Composition and Functional Group Studies

The EDS spectra as shown in Fig. 1c revealed the presence of four elements, including Na, Y, F, and Eu. This provided further proof that the prepared sample was $NaYF_4:Eu$, which is also verified by XRD analysis. The results were validated, showing that Eu was dispersed inside $NaYF_4$ uniformly and was well-doped. Additionally, the weight and atomic percentages of the different elements are included in the inset of EDS graph.

Figure 1d shows the FTIR spectrum of the prepared nanoparticles in the wavenumber range of 500–4000 cm^{-1}. The broad band centered at around 3109 cm^{-1} could be related to the O–H stretching vibration [22]. A small absorption peak at 2821 cm^{-1} was observed that verifies the presence of symmetric vibrations of CH_2 stretching modes [23]. A weak band at 2006 cm^{-1} is related to the C-H stretching mode. The vibration of the carboxylic group is responsible for the occurrence of peaks at around 1752 cm^{-1} and 1400 cm^{-1}. The peak at 1079 cm^{-1} corresponds to C-O stretching mode. In the measured range, there is no observable vibrational peak attributable to the host lattice $NaYF_4$.

Fig. 1 a XRD, **b** FESEM, **c** EDS, and **d** FTIR of NaYF$_4$:Eu nanoparticles
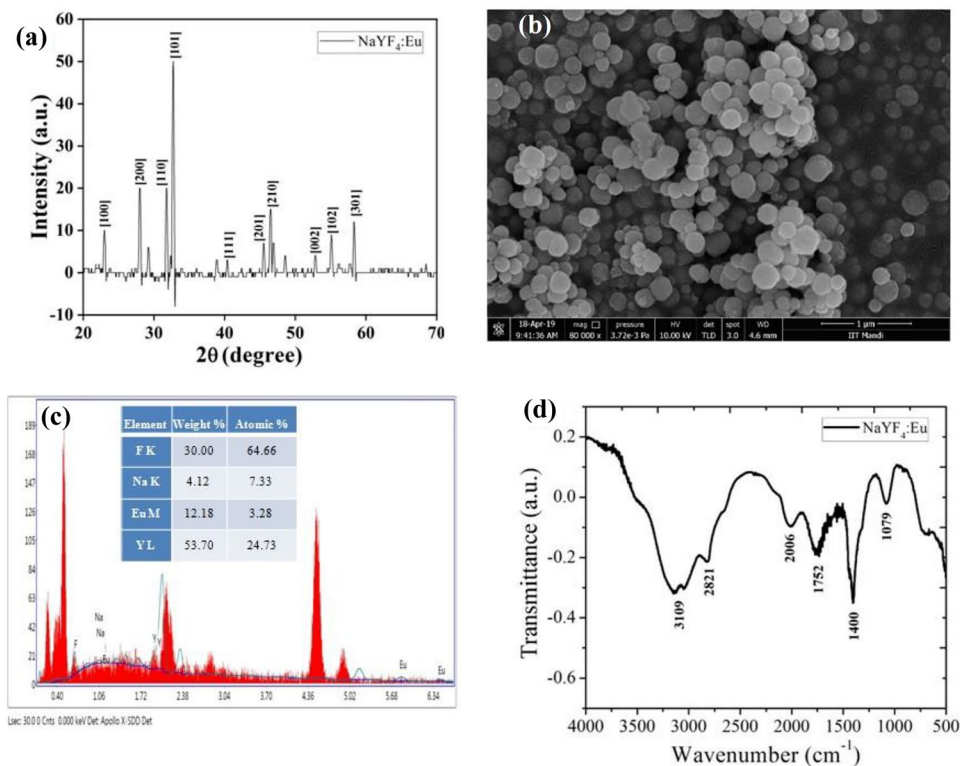
3.4 Synthesis of NaYF$_4$:Eu Deposited Paper-Based Colorimetric Sensors

Firstly, eight different solutions were prepared by dissolving 0.15 g of each of the eight chosen chemicals (i.e., 1-Cd(NO$_3$)$_2$, 2-Mg(CH$_3$COO)$_2$·4H$_2$O, 3-PbCO$_3$, 4-Co(NO$_3$)$_2$, 5-MoO$_3$, 6-Cu(CH$_3$COO)$_2$, 7-Ni(NO$_3$)$_2$·6H$_2$O, and 8-C$_4$H$_6$MnO$_4$) in distilled water (50 mL). Some chemicals dissolved completely in DI water after heating. Afterwards, a piece of photo paper was taken, and the solution of NaYF$_4$:Eu (0.1 g) with ethanol (20 mL) was deposited on it. After 2 h, the samples were completely stuck with the paper. Forty milliliters of each solution was added on the uncoated and NaYF$_4$:Eu-coated paper. Out of eight, two metals showed significant change in color (4-Co^{+2}, 6-Cu^{+2}), and for the remaining two metals, less change in color (5-Mo^{+4}, 8-Mn^{+2}) on the paper is observed which is shown in Fig. 2a. Out of four metal solutions which show change in color, we make six combinations of solution by mixing two, four combinations by mixing three, and one combination by mixing all four, which is clearly shown in Fig. 2b–d, respectively. The combination of different metal ions is shown in Table S1 (Supplementary Information). It is observed that in all the combinations, the color of uncoated paper is significantly different from the NaYF$_4$:Eu-coated paper when we add 40 mL of each solution on different piece of paper.

3.5 UV–vis Analysis

We proceeded to examine the variance in color change that occurs to different metal ions in a solution of DI water using a UV–vis spectrometer. The band illustrated in Fig. 3 was assignable to intermolecular charge-transfer transitions due to the addition of NaYF$_4$:Eu in the solution of various metal salt in DI water. It was noticed that a wide range of spectral modifications, as well as different color transformations, occurred when Mn^{+2} and Mo^{+4} were added. It should be noted that the absorbance changes as a result of these two metal ions were quite different from one another. The UV–vis analysis of Cu^{+2} and Co^{+2} is not required because the color change is directly observed through naked eyes.

Fig. 2 Photographs of the test strips of NaYF$_4$:Eu-deposited paper-based colorimetric sensors for the visual detection of Cu^{+2}, Mn^{+2}, Co^{+2}, and Mo^{+4}. (**a**) shows all the 8 combinations of solutions; (**b**) shows 6 combinations by mixing two solutions; (**c**) 4 combinations by mixing three solutions; and (**d**) shows 1 combination by mixing four solutions as indicated in Table S1
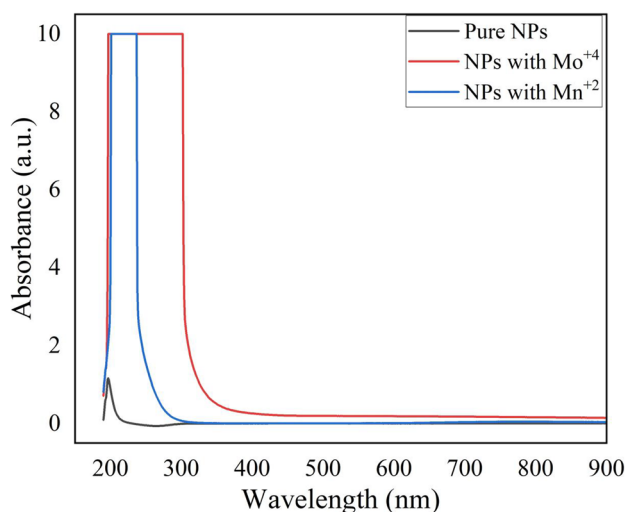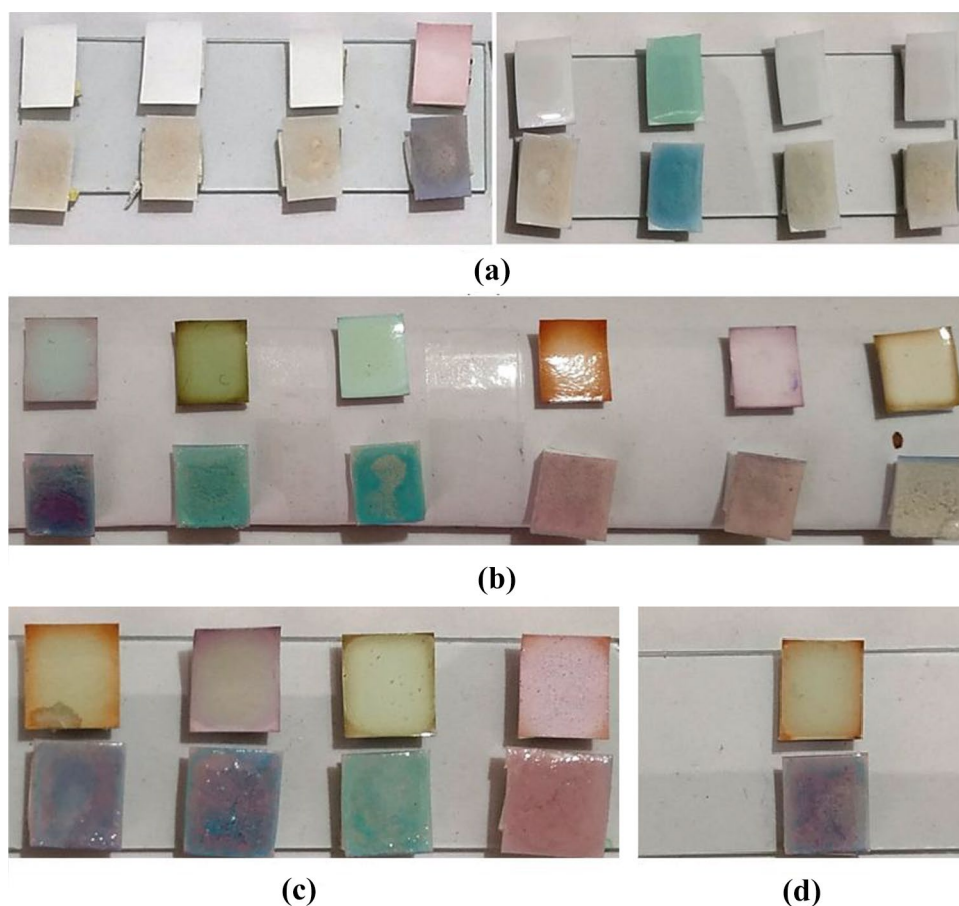

(a)

(b)

(c)   **(d)**

Fig. 3 UV–vis spectra of NaYF$_4$:Eu (20 μL from 0.1 g in 20 mL) in DI water in the presence of fix concentrations of Mn^{+2} and Mo^{+4}

FESEM, EDS, and FTIR. As an attempt of visual field detection, simple test strips have been successfully developed over which NaYF$_4$:Eu nanoparticles were deposited, and these strips were applied to visual monitoring of four metal ions (viz. Cu^{+2}, Mn^{+2}, Co^{+2}, and Mo^{+4}) by the naked eye. The developed sensor possesses good selectivity and sensitivity. This study indicates a significant potential for on-site rapid water quality analysis using NaYF$_4$:Eu^3 nanoparticles.

Declarations

4 Conclusions

We have successfully synthesized NaYF$_4$:Eu nanoparticles via sol–gel method. The prepared nanoparticles were then characterized using characterization techniques like XRD,

References

1. S.S. Dhaliwal, J. Singh, P.K. Taneja, A. Mandal, Remediation techniques for removal of heavy metals from the soil contaminated through different sources: a review. Environ. Sci. Pollut. Res. **27**(2), 1319–1333 (2020)

2. B. Wei, L. Yang, A review of heavy metal contaminations in urban soils, urban road dusts and agricultural soils from China. Microchem. J. **94**(2), 99–107 (2010)

3. S. Muhammad, M.T. Shah, S. Khan, Health risk assessment of heavy metals and their source apportionment in drinking water of Kohistan region, northern Pakistan. Microchem. J. **98**(2), 334–343 (2011)

4. F.W. Ntengwe, Pollutant loads and water quality in streams of heavily populated and industrialised towns. Physics and Chemistry of the Earth, Parts A/B/C **31**(15–16), 832–839 (2006)

5. A.K. Krishna, M. Satyanarayanan, P.K. Govil, Assessment of heavy metal pollution in water using multivariate statistical techniques in an industrial area: a case study from Patancheru, Medak District, Andhra Pradesh, India. J. Hazard. Mater. **167**(1–3), 366–373 (2009)

6. M.S. Bhuyan, M.A. Bakar, M. Rashed-Un-Nabi, V. Senapathi, S.Y. Chung, M.S. Islam, Monitoring and assessment of heavy metal contamination in surface water and sediment of the Old Brahmaputra River, Bangladesh. Appl Water Sci **9**(5), 1–13 (2019)

7. Q. Wang, Q. Huang, Q. Guo, J. Qin, J. Luo, Z. Zhu, Y. Hong, Y. Xu, S. Hu, W. Hu, C. Yang, Reducing bioavailability of heavy metals in contaminated soil and uptake by maize using organic-inorganic mixed fertilizer. Chemosphere **261**, 128122 (2020)

8. H. Qin, T. Hu, Y. Zhai, N. Lu, J. Aliyeva, The improved methods of heavy metals removal by biosorbents: a review. Environ. Pollut. **258**, 113777 (2020)

9. J.H. Duffus, "Heavy metals" a meaningless term?(IUPAC Technical Report). Pure Appl. Chem. **74**(5), 793–807 (2002)

10. F. Li, Z. Qiu, J. Zhang, W. Liu, C. Liu, G. Zeng, Investigation, pollution mapping and simulative leakage health risk assessment for heavy metals and metalloids in groundwater from a typical brownfield, middle China. Int. J. Environ. Res. Public Health **14**(7), 768 (2017)

11. M. Jaishankar, T. Tseten, N. Anbalagan, B.B. Mathew, K.N. Beeregowda, Toxicity, mechanism and health effects of some heavy metals. Interdiscip. Toxicol. **7**(2), 60 (2014)

12. L. Järup, Hazards of heavy metal contamination. Br. Med. Bull. **68**(1), 167–182 (2003)

13. A.G. Khan, Promises and potential of in situ nano-phytoremediation strategy to mycorrhizo-remediate heavy metal contaminated soils using non-food bioenergy crops (Vetiver zizinoides & Cannabis sativa). Int. J. Phytorem. **22**(9), 900–915 (2020)

14. R.C. Machado, D.F. Andrade, D.V. Babos, J.P. Castro, V.C. Costa, M.A. Sperança, J.A. Garcia, R.R. Gamela, E.R. Pereira-Filho, Solid sampling: advantages and challenges for chemical element determination—a critical review. J. Anal. At. Spectrom. **35**(1), 54–77 (2020)

15. T. Rasheed, S. Shafi, M. Bilal, T. Hussain, F. Sher, K. Rizwan, Surfactants-based remediation as an effective approach for removal of environmental pollutants—a review. J. Mol. Liq. 113960 (2020)

16. X. Tian, L. Chen, Y. Li, C. Yang, Y. Nie, C. Zhou, Y. Wang, Design and synthesis of a molecule with aggregation-induced emission effects and its application in the detection of arsenite in groundwater. Journal of Materials Chemistry C **5**(15), 3669–3672 (2017)

17. M.R. Awual, M.M. Hasan, Colorimetric detection and removal of copper (II) ions from wastewater samples using tailor-made composite adsorbent. Sens. Actuators, B Chem. **206**, 692–700 (2015)

18. N. Fleck, H. Amli, V. Dhanak, W. Ahmed, Characterization techniques in energy generation and storage. In Micro and Nano Technologies, *Emerging Nanotechnologies for Renewable Energy*, (Elsevier, 2021), pp. 259–285

19. A. Ahmed, A. Singh, A. Sharma, S. Verma, S. Mahajan, S. Arya, Investigating the thermographical effect on optical properties of Eu doped Y2O3: TiO2 nanocomposite synthesized via sol-gel method. Solid State Sci. **116**, 106617 (2021)

20. M. Banski, M. Afzaal, A. Podhorodecki, J. Misiewicz, A.L. Abdelhady, P. O'Brien, Passivation of lanthanide surface sites in sub-10 nm NaYF 4: Eu 3+ nanocrystals. J. Nanopart. Res. **14**(11), 1–10 (2012)

21. P. Mahajan, A. Singh, R. Datt, V. Gupta, S. Arya, Realization of inverted organic solar cells by using sol-gel synthesized ZnO/Y 2 O 3 core/shell nanoparticles as electron transport layer. IEEE Journal of Photovoltaics **10**(6), 1744–1749 (2020)

22. F. Cheng, Q. Cao, Y. Guan, H. Cheng, X. Wang, J.D. Miller, FTIR analysis of water structure and its influence on the flotation of arcanite (K2SO4) and epsomite (MgSO4·7H2O). Int. J. Miner. Process. **122**, 36–42

23. A. Singh, S. Arya, M. Khanuja, A.K. Hafiz, R. Datt, V. Gupta, A. Khosla, Eu doped NaYF 4@ Er: TiO 2 nanoparticles for tunable ultraviolet light based anti-counterfeiting applications. Microsyst. Technol. 1–10 (2020)